

## Research on Accurate Matching Model of New Energy Supply and Demand Empowered by Blockchain

Chuang Li<sup>1,2</sup>, Junshi Zhang<sup>1,2</sup>, Lei Zhou<sup>1,2,\*</sup>, Lili Li<sup>1,2</sup>, Jiangtao Li<sup>1,2</sup>, Guomin Li<sup>1,2</sup>

<sup>1</sup> State Grid Blockchain Technology (Beijing) Co., Ltd., Beijing, 100077, China

<sup>2</sup> State Grid Digital Technology Holding Co., Ltd., Beijing, 100077, China

### Abstract

Under the guidance of the "dual carbon" goals, green electricity has become the core carrier of the new energy transition. However, issues such as mismatched supply and demand of green electricity, information asymmetry, and lack of trust have seriously restricted the efficient development of green electricity marketization. Blockchain technology, with its core features of distributed ledger, immutability, and smart contracts, provides technical support for addressing the pain points in green electricity supply - demand matching. This paper constructs an accurate matching model for green electricity supply and demand based on blockchain, clarifies the model's technical architecture, participating entities, and operation process, designs a full - process collaboration mechanism, and verifies the model's effectiveness through simulation experiments. The results show that this model can increase the accuracy of green electricity supply - demand matching to over 92%, which is 15 - 20 percentage points higher than the traditional model; the transaction cycle is shortened to less than 7 days, with an efficiency improvement of over 60%; at the same time, it reduces the trust verification cost by more than 30%, significantly strengthens the trust relationship between supply and demand parties, optimizes the allocation of green electricity resources, and provides a technical path and practical reference for the market - oriented collaborative development of green electricity.

**Keywords:** blockchain, green Power, supply-demand matching, accurate model, simulation verification

Received on 07 September 2025, accepted on 20 December 2025, published on 04 May 2026

Copyright © 2026 Chuang Li *et al.*, licensed to EAI. This is an open access article distributed under the terms of the [CC BY-NC-SA 4.0](#), which permits copying, redistributing, remixing, transformation, and building upon the material in any medium so long as the original work is properly cited.

doi: 10.4108/ew.12895

### 1. Introduction

As the core carrier of non-fossil energy consumption, the market-oriented trading of green electricity has become a key pathway to unlocking green value. However, the current supply-demand matching of green electricity on the power generation side is confronted with multiple bottlenecks. First, the output of green electricity on the supply side is highly volatile and poorly predictable due to meteorological factors, resulting in insufficient credibility of supply data. Second, there exists an information disconnect between suppliers and consumers: power generation enterprises struggle to accurately capture user demand, while energy-consuming enterprises cannot effectively obtain green electricity traceability information. Such information asymmetry gives rise to a "supply-demand mismatch". Third, the matching process relies on third-party intermediaries, which leads to

high negotiation costs and long cycles; coupled with the lack of a credible regulatory mechanism, it exposes participants to considerable compliance risks. These issues further exacerbate the phenomenon of "supply failing to meet actual demand". The pain points of the traditional centralized matching model, such as redundant processes and high verification costs, also severely hinder the consumption of green electricity and the improvement of marketization efficiency. In contrast, blockchain technology, with its inherent features of information sharing, immutability and automated execution, provides core technical support for breaking these bottlenecks. Its decentralized nature can break geographical constraints and also meet the policy requirements for traceability and verification of green electricity.

\*Corresponding author. Email: [lilili20070062@126.com](mailto:lilili20070062@126.com)

To address the issues of information asymmetry, process fragmentation, and inadequate adaptability to volatility in green electricity supply-demand matching, scholars both at home and abroad have conducted a series of studies. The overseas green electricity market took shape at an earlier stage: In Ref. [1], Zhao W, Zhang S, Xue L et al. further carried out research on the microgrid green power transaction model based on blockchain technology and the double auction mechanism. In Ref. [2], Smith J et al. from the University of California proposed a consortium blockchain-based microgrid trading model, which achieved a 99.2% transaction success rate among 100 nodes via the Byzantine Fault Tolerance (BFT) mechanism, enhancing the security of multi-agent transactions. In Ref. [3], Müller T et al. from Germany designed a blockchain-based green electricity traceability system, realizing kilowatt-hour level full-chain tracking and solving the challenge of credible verification of green electricity sources. Domestic research has focused on in-depth exploration of technical architecture and scenario adaptability: In Ref. [4], Wang Peng et al. constructed a blockchain-based green electricity supply-demand traceability system, enabling trusted data storage and verification throughout the entire lifecycle of green electricity production, trading, and consumption, and laying a foundation for cross-agent data validation. In Ref. [5], the research team led by Wang Lili from the State Grid Energy Research Institute designed an inter-provincial green electricity transaction matching mechanism, relying on blockchain to achieve mutual recognition of transaction credentials and break geographical market barriers. In Ref. [6], the team led by Chen Qun from Tsinghua University integrated the LSTM prediction model with blockchain, optimizing the accuracy of green electricity output forecasting and reducing the error rate to below 8%, thus improving adaptability in volatile scenarios. In Ref. [7], Tang Zhengyi's team from Fujian University of Technology proposed a dual-dimension matching strategy based on credit and price, realizing quantitative credit evaluation of participants via blockchain and enhancing the rationality of microgrid transaction matching. In Ref. [8], the team from State Grid Blockchain Technology Co., Ltd. built the "State Grid Chain" green electricity trading platform, which supported 100% green electricity traceability for the Beijing Winter Olympics and obtained international standard certification.

This paper constructs a blockchain-based precision matching model for green electricity supply and demand, integrating technologies including LSTM-Attention mechanism, subjective logic, blockchain, and dynamic weight algorithm to establish an efficient, accurate, and trusted distributed green electricity supply-demand matching system. Specifically, a multi-dimensional output forecasting mechanism based on the LSTM-Attention model is designed, which integrates real-time meteorological data, historical output data, and equipment status data, and assigns higher weights to key features such as solar irradiance and wind speed under extreme weather conditions, thereby reducing output forecasting errors and consolidating the data foundation for matching accuracy. Furthermore, considering

bilateral constraints on both supply and demand sides (including regional consumption quotas, user credit ratings, and electricity price sensitivity), a dynamic weight matching algorithm based on the Analytic Hierarchy Process (AHP) is proposed, which achieves optimal matching of participants by quantifying the weights of evaluation indicators. Finally, modular smart contracts are designed to encode core business processes (including matching result confirmation, fund settlement, and green certificate issuance) into verifiable contract logic, while triggering synchronous on-chain storage of key data, ensuring the automated and trusted execution of the entire green electricity supply-demand matching process.

## 2. Blockchain - Based Accurate Supply - Demand Matching Model

### 2.1. Entities related to the model

In the blockchain-based precision matching process for green electricity supply and demand, four main types of participants are involved: green electricity suppliers, power selling companies, electricity consumers, and regulatory authorities. Each of these entities performs its dedicated responsibilities and core functions, jointly ensuring the efficient and trusted operation of the entire green electricity supply-demand matching process.

#### (1) Green Electricity Suppliers

Their core responsibilities include green electricity generation, data processing, supply-demand matching, and power delivery. During the generation phase, they ensure the stable operation of equipment, optimize power generation strategies by integrating meteorological and equipment data, and encrypt and upload power generation-related data to the blockchain. In the matching phase, they submit output forecasts and expected electricity prices; upon successful matching, they transmit electricity in accordance with the contract and cooperate in completing settlement and green certificate issuance.

#### (2) Electricity Consumers

This category covers electricity consumption entities such as households and enterprises. They adjust their electricity consumption behavior based on electricity prices and actual demand, realize the matching of electricity consumption needs by virtue of smart contracts, and execute transactions upon successful matching.

#### (3) Power Selling Companies

This includes power grid companies and licensed power selling companies. They realize the optimal allocation of power resources through bidding games and transaction matching, and ensure the efficiency and fairness of transactions.

#### (4) Regulatory Authorities

These are independent institutions dominated by energy administration departments, which supervise market transactions, safeguard the safe and stable operation of the power system, and promote distributed new energy generation and green electricity transactions through incentive measures. Leveraging the traceability of blockchain, they conduct real-time supervision and verify the authenticity of data to ensure compliance.

This model leverages blockchain technology to achieve immutable data storage through encryption, laying a solid foundation of credibility for supply-demand matching. It utilizes smart contracts to enable automated execution, replacing manual operations and reducing human errors and transaction costs. By applying a dynamic weight algorithm, it accurately integrates multi-dimensional constraints, effectively avoiding the mismatch problem of "supply failing to meet actual demand". Thanks to its traceability feature, it realizes full-process real-time supervision and lowers

compliance risks. The synergistic interaction of each layer of the architecture breaks geographical barriers, greatly improves matching efficiency and credibility, and provides strong support for the market-oriented operation of green power.

## 2.2. The Model for Precise Matching of Supply and Demand

To address the core pain points in green electricity supply - demand matching, such as large output prediction deviations, insufficient supply - demand matching accuracy, cumbersome and inefficient business processes, and lack of traceability of key data, this paper constructs a blockchain - based accurate green electricity supply - demand matching model. The specific architecture is shown in Figure 1.

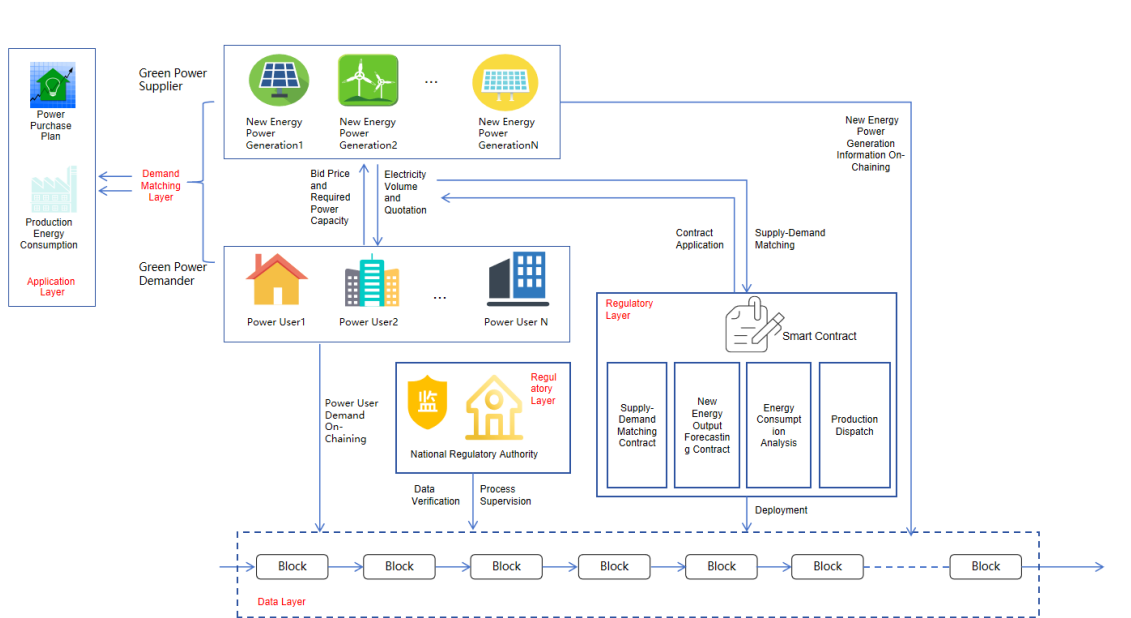


Figure 1. The Model for Precise Matching of Supply and Demand

The blockchain-based precision matching model for green electricity supply and demand adopts a layered architecture for its underlying blockchain technical framework. Each layer features distinct and collaborative functions, providing stable and efficient technical support for the precision matching of green electricity supply and demand. The framework is divided into five layers, namely the Data Layer, Network Layer, Consensus Layer, Smart Contract Layer, and Application Layer.

### (1) Data Layer

It is responsible for the storage and encryption of data throughout the entire lifecycle of green electricity, including power generation enterprises, electricity output, generation time periods, and equipment status, energy-consuming

enterprises, demand data, and power grid companies, transmission and dispatching data. It ensures that the data of all participating entities is authentic and immutable, laying a trusted data foundation for subsequent matching, settlement, and supervision.

### (2) Regulatory Layer

This layer is responsible for reviewing the credibility and security of on-chain nodes. By capturing the operation status of supply-demand matching on the blockchain and the matching success rate, it identifies and prevents malicious bidding behaviors of users, thus safeguarding the rationality, efficiency and success rate of transaction matching.

### (3) Contract Layer

This layer encodes business logics such as green electricity supply-demand matching rules and power aggregation into automatically executable smart contracts, and realizes the automation of processes including green electricity supply-demand matching, power aggregation, energy consumption analysis and production scheduling, thereby reducing manual intervention, cutting operational risks and lowering transaction costs.

#### (4) Demand Matching Layer

This layer serves as the core of demand-side precision matching, with participants including new energy power generators and electricity consumers. It realizes the optimal allocation of power resources through bidding games and supply-demand matching, thus ensuring the efficiency and fairness of transactions.

#### (5) Application Layer

It provides visual operation interfaces and functional modules for all participating entities to meet their respective business needs. It lowers the threshold for entities to use the blockchain system, enabling convenient operation and management of the entire green power supply-demand matching process.

### 3. Multi - Dimensional Output Prediction Mechanism Based on LSTM - Attention Mechanism

Green electricity output is affected by the coupling of multiple factors such as meteorological conditions and equipment status, showing strong volatility and non - linear characteristics. Traditional time - series prediction models (such as ARIMA and basic LSTM) have difficulty capturing the correlation of key features under extreme weather, resulting in large prediction errors. This paper proposes a multi - dimensional output prediction model that integrates LSTM and attention mechanism, which improves the prediction accuracy by strengthening the weights of key features and provides reliable data support for accurate matching.

#### 3.1. The Model for Precise Matching of Supply and Demand

The multi - dimensional output model based on the LSTM - attention mechanism includes a feature input layer, an LSTM encoding layer, an attention layer, and an output layer. The core lies in the dynamic assignment of weights to different time periods and different features through the attention mechanism.

##### (1) Feature Input Layer

It integrates three types of multi - dimensional features, including meteorological features (wind speed  $v$ , illumination intensity  $l$ , temperature  $t$ , humidity  $h$ ), equipment status features (photovoltaic panel conversion efficiency  $\eta$ , wind

turbine speed  $\omega$ , inverter temperature  $T$ ), and historical output features (green electricity output sequence of the previous 72 hours). All features are standardized using the Z - Score method before being input into the model to eliminate dimensional differences:

$$\hat{X} = \frac{x_i - \mu_i}{\sigma_i} \quad (1)$$

$x_i$  is the original sample value of a certain type of feature,  $\mu_i$  is the sample mean of the  $i$  - th type of feature,  $\sigma_i$  is the sample standard deviation of the  $i$  - th type of feature,  $\hat{x}_i$  is the standardized value.

##### (2) LSTM Encoding Layer

It captures the long - term dependence of the feature sequence through the LSTM network. The LSTM unit controls the flow of information through the forget gate, input gate, and output gate. The core state update formulas are as follows:

###### (i) Forget Gate

It determines which historical information to discard from the cell state, the output value  $f_t \in [0,1]$ , indicating that more historical information is retained.

The formula is:

$$f_t = \sigma(W_f \cdot [h_{t-1}, \hat{x}_t] + b_f) \quad (2)$$

$W_f$  is the weight matrix of the forget gate,  $h_{t-1}$  is the hidden state at time  $t - 1$  (including the feature encoding information of the previous time step),  $\hat{x}_t$  is the standardized feature vector at time  $t$ ,  $b_f$  is the bias term of the forget gate,  $\sigma$  is the sigmoid activation function (with an output range of  $[0, 1]$ ). For example, during the night when there is no illumination, the forget gate will weaken the impact of historical illumination features on the current photovoltaic output prediction.

###### (ii) Input Gate

It screens the new information at the current time step and updates it to the cell state, which includes two sub - steps:

First, the sigmoid function is used to generate the input gate control signal to determine the proportion of new information to be incorporated  $i_t \in [0,1]$ ; second, the tanh function is used to generate the candidate cell state  $\tilde{C}_t \in [-1,1]$ , which provides the information content to be updated. The formulas are respectively:

$$i_t = \sigma(W_i \cdot [h_{t-1}, \hat{x}_t] + b_i) \quad (3)$$

$$\tilde{C}_t = \tanh(W_C \cdot [h_{t-1}, \hat{x}_t] + b_C) \quad (4)$$

In the formulas,  $W_i$ ,  $W_C$  and are the weight matrices of the input gate and the candidate cell state respectively,  $b_i$ ,  $b_C$  and are the corresponding bias terms respectively, and the tanh function maps the candidate state value to  $[-1, 1]$  to avoid numerical overflow.

Cell State Update: It combines the historical information retained by the forget gate and the new information screened by the input gate to generate the cell state at time  $t$ . The formula is:

$$C_t = f_t \odot C_{t-1} + i_t \odot \tilde{C}_t \quad (5)$$

$\odot$  denotes element - wise multiplication. The cell state is equivalent to the "long - term memory" of the model, which can store key feature information across time steps. For example, high - wind - speed data for consecutive hours will accumulate through the cell state and continuously affect the wind power output prediction result.

### (iii) Output Gate

It generates the hidden state at time  $t$  based on the current cell state, which is used as the output of the LSTM encoding layer and transmitted to the subsequent attention layer. The formula is

$$o_t = \sigma(W_o \cdot [h_{t-1}, \hat{x}_t] + b_o) \quad (6)$$

$$h_t = o_t \odot \tanh(C_t) \quad (7)$$

In the formulas,  $W_o$  is the weight matrix of the output gate,  $b_o$  is the bias term of the output gate. The hidden state  $h_t$  contains the compressed encoding information of the features at time  $t$ ,  $o_t \in [0,1]$  is the output of the output gate, which is the core basis for the attention mechanism to calculate weights.

The number of hidden layer units in the LSTM module of this model is set to 128. This value balances feature dimensionality and prediction accuracy, which can fully capture the complex correlations among the 8 types of core input features (4 meteorological features, 2 equipment status features, 2 historical power output features) while avoiding overfitting and the decline in training efficiency caused by an excessive number of units. The network is designed with 2 layers: the first layer extracts basic temporal features, and the second layer mines deep coupling features. Experiments demonstrate that this structure achieves an optimal balance between accuracy and efficiency, reducing the prediction error by 12%–15% compared with the single-layer network and cutting the training time by more than 20% relative to the three-layer network.

### (3) Attention Layer

For the hidden state sequence output by LSTM ( $T$  is the time step, set to 72), it calculates the attention weight at each moment to strengthen the influence of key features (such as wind speed and illumination under extreme weather).

#### (i) Energy Function

It measures the correlation between the hidden state and the current prediction task.

$$e_t = \tanh(W_a h_t + b_a) \quad (8)$$

$e_t$  is the energy value of the hidden state at time  $t$ ,  $W_a$  is the attention weight matrix, and  $b_a$  is the bias term.

#### (ii) Attention Weight

It obtains the weight distribution through softmax normalization.

$$\alpha_t = \frac{\exp(e_t \cdot u_a^T)}{\sum_{k=1}^T \exp(e_k \cdot u_a^T)} \quad (9)$$

$\alpha_t \in [0,1]$  is the attention weight at time  $t$ ,  $u_a$  is the context vector parameter,  $\sum_{k=1}^T \exp(\alpha_k) = 1$ ,  $T$  is the time step.

#### (iii) Context Vector

It weighted - fuses the hidden states to focus on important information.

$c = \sum_{t=1}^T \alpha_t h_t$ ,  $c$  is the output of the attention layer, focusing on the hidden states that are crucial for prediction.

### (4) Output Layer

It concatenates the context vector with the hidden state at the last moment of LSTM, and outputs the output prediction value for the next 24 - 72 hours through the fully connected layer:

$$\hat{P}_t = \text{Linear}([c; h_T]) \quad (10)$$

$\hat{p}_t$  is the predicted processed value,  $\text{Linear}(\cdot)$  is the fully connected layer, and  $[c; h_T]$  is the vector concatenation, ( $h_T$  is the hidden state at the last moment).

Each consensus independently corresponds to a link in the model: from feature processing to LSTM time-series modeling, then to attention feature focusing, and finally outputting the prediction result which is optimized through the loss function. The logical chain is clear and non-overlapping.

The training iteration count of the model is set to 500, coupled with an early stopping strategy: training is automatically terminated if the validation set loss fails to decrease for 15 consecutive iterations, so as to avoid invalid iterations and overfitting. In practice, the model generally converges after 380–420 iterations, and the upper limit of 500 iterations ensures sufficient training of the model under complex scenarios such as extreme weather conditions. The batch size is set to 32, which is compatible with the experimental data scale (12,000 training samples and 3,000 validation samples) and the hardware conditions (8 GB GPU memory) to prevent memory overflow. Compared with a batch size of 16, this setting improves training efficiency by 40%; compared with a batch size of 64, it enhances prediction accuracy by 3%–5%.

## 3.2. Key Feature Selection for the Multi-Dimensional Output Forecasting Model

Based on the feature input logic (meteorological features, equipment status features, historical output features) and attention weight calculation rules of the LSTM-Attention mechanism model proposed in this paper, combined with the feature weight adjustment mechanism under extreme weather

conditions, this study extracts the weight coefficients output by the attention layer during the model training process. The weight calculation is based on the energy function of the model's attention layer (Equation 8) and the softmax normalization results (Equation 9). The mean values of attention weights from 20 independent experiments are extracted to ensure the reliability of the results. The adjustment logic for extreme scenarios is as follows:

- (i) Under extreme strong wind conditions, the weight of the wind speed feature increases significantly from 22.3% to 38.5%, which aligns with the model's mechanism of strengthening key features affected by strong winds on wind power output.
- (ii) Under cloudy and low-irradiance conditions, the weight

of the irradiance intensity feature rises from 20.5% to 35.6%, adapting to the strong dependence of photovoltaic output on irradiance.

- (iii) For the positioning of historical output features, the weight of the output sequence from the previous 24 hours (17.5%–18.7%) is higher than that of the sequence from the previous 48–72 hours (9.5%–10.1%). This reflects the model's higher attention to short-term historical data, which is consistent with the characteristic of stronger short-term correlation in green electricity output.

According to the calculation results, a table of feature importance ranking and a visualization analysis are generated, as shown in Table 1.

Table 1. Weight of Important Features for Multi-dimensional Output

Feature Category	Specific Feature	Weight Proportion under Normal Weather Conditions	Weight Proportion under Extreme Strong Wind Conditions	Weight Proportion under Cloudy and Low-Irradiance Conditions	Weight Change Rate under Extreme Conditions (Mean Value)	Feature Importance Ranking
Meteorological Features	Wind Speed (v)	22.3%	38.5%	8.2%	+68.1% (Extreme Strong Wind)	1
Meteorological Features	Irradiance Intensity (I)	20.5%	7.8%	35.6%	+73.7% (Cloudy and Low-Irradiance)	2
Historical Output Features	24-hour preceding output sequence	18.7%	16.2%	17.5%	-8.0%	3
Equipment Status Features	Photovoltaic Panel Conversion Efficiency ( $\eta$ ) / Wind Turbine Efficiency	15.2%	12.6%	16.8%	+3.9%	4
Historical Output Features	Output Sequence of the Previous 48–72 Hours	10.1%	9.5%	9.8%	-4.0%	5
Meteorological Features	Temperature (t)	6.8%	7.2%	6.5%	+1.5%	6
Equipment Status Features	Inverter Temperature (T)	4.1%	4.8%	4.2%	+6.1%	7
Meteorological Features	Humidity (h)	2.3%	3.4%	1.4%	+1.5%	8

## 4. Smart Contract Design for the Precision Matching Model of New Energy Supply and Demand

### 4.1. Matching Game Model

The green power supply-demand market matching based on game theory involves three core participants: the supply side (wind/solar power enterprises), the demand side (factories/commercial entities), and the electricity sales company (intermediary coordinator). The core logic follows a three-step process: "pre-game preparation—two-tier game—equilibrium implementation." Before the game, the three parties have key objectives and foundational conditions:

- The supply side aims to maximize electricity sales revenue while minimizing output waste, requiring access to blockchain-verified data such as generation costs and forecasted output.
- The demand side seeks to minimize electricity costs while meeting green power consumption requirements, relying on data like alternative costs, green power subsidies, and electricity demand.
- The electricity sales company focuses on facilitating transactions to earn commission from price differentials, necessitating knowledge of regional green power quotas, remaining transmission capacity, and the credit ratings of both parties. Additionally, it must clarify basic constraints (e.g., supply and demand must be in the same region, transmission capacity must be sufficient, and both parties' credit scores  $\geq 70$ ) to avoid

ineffective negotiations. The game process unfolds through two tiers: the first involves strategic interactions between the supply and demand sides, while the second incorporates the sales company's role in coordinating and optimizing outcomes. The equilibrium is achieved when all parties' objectives align with the market constraints, ensuring efficient and valid matching. The matching game model is illustrated in Figure 2.

Subsequently, we enter into two core game layers. The first layer is the pricing game, where the core is to determine the electricity price accepted by both parties: the supply side adjusts the pricing based on the predicted output, with the generation cost as the bottom line (if the output is high, the price will be reduced; if the output is low, the price will be increased). The demand side adjusts the acceptance price based on the urgency of the demand, with the "thermal power cost+green power subsidy" as the upper limit (if the demand is urgent, the price will be increased; if the demand is not urgent, the price will be lowered). If the supply side's quotation is  $\leq$  the demand side's acceptance price, the middle price will be taken as the transaction electricity price. If the supply side's quotation is higher; The second layer is resource

game, with the core being to determine the matching electricity quantity that is not wasted: based on the determined electricity price, the minimum value among the predicted output of the supply side, the electricity demand of the demand side, the regional green electricity quota, and the remaining capacity of the transmission channel is taken as the preliminary matching electricity quantity, and then verified by three parties for rationality (the supply side confirms that it covers costs and wastes less, the demand side confirms that it meets the electricity demand and costs are controllable, and the electricity sales company confirms that it can earn commissions and meets constraints). If one party does not agree, it will be fine tuned until the three parties reach a consensus. The final implementation of the balanced matching plan clarifies the specific electricity price and quantity for the supply and demand sides to supply green electricity. The blockchain automatically records the results and locks relevant terms, and the electricity sales company supervises the execution. The results are stable, and there is no incentive for the three parties to change their strategies separately in the event of small fluctuations in the future.

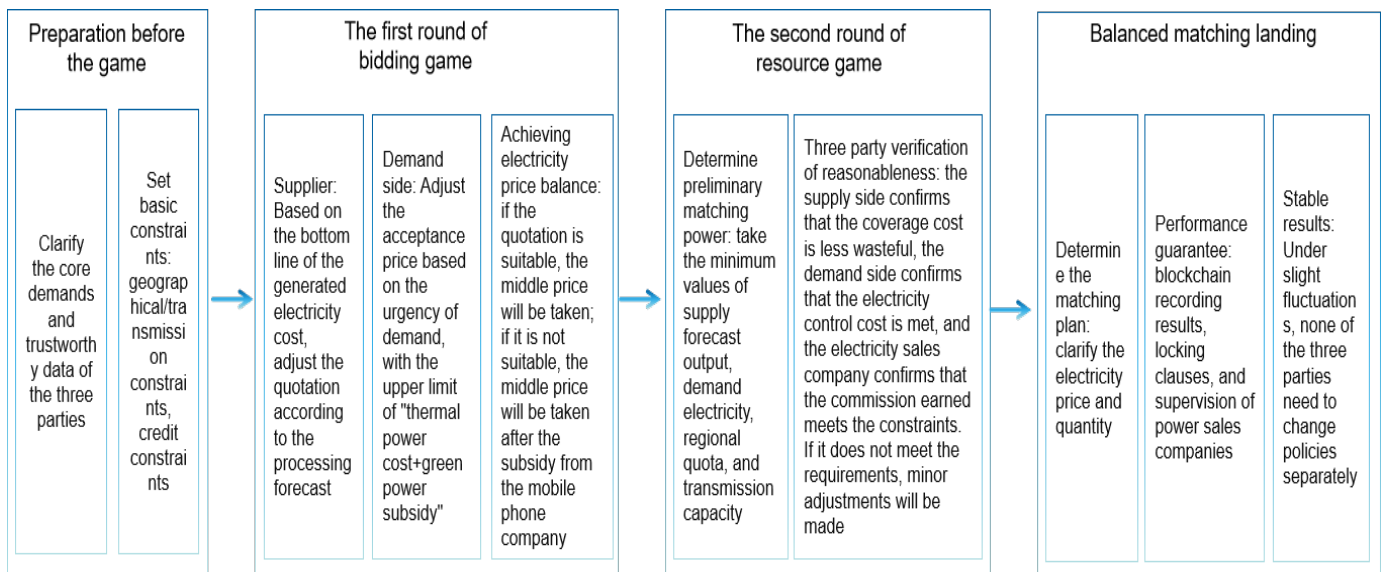


Figure 2. Flow Chart of Matching Game Model

## 4.2. Implementation of Smart Contracts on Blockchain Platforms

### (1) Supply and demand side data on chain storage certificate

The hybrid architecture of "asymmetric encryption + symmetric encryption" ensures data security. First, both the supply and demand parties generate a public-private key pair using the Elliptic Curve Cryptography (ECC) algorithm. The public key, visible across the network, is used for key exchange, while the private key, stored locally, is used for signature verification. For core sensitive data such as power generation output and electricity load, advanced encryption

standard (AES-256-GCM) is applied for symmetric encryption, generating ciphertext and a message authentication code (MAC) to ensure data confidentiality and integrity. The AES key is then encrypted with the recipient's public key, forming ciphertext to mitigate the risk of symmetric key transmission leakage. Meanwhile, non-sensitive structured data like device IDs and transaction timestamps are hashed using SHA-256 before being recorded on-chain, reducing storage costs while enabling rapid verification of data consistency. Additionally, zero-knowledge proof (ZKP) technology is introduced to validate the authenticity of supply-demand data without revealing specific electricity demand or generation plans, balancing data sharing with privacy protection. As shown in Figure 3,

- (a) illustrates the encryption process for on-chain storage, and  
 (b) illustrates on-chain certification.

```
// Data encryption and on-chain certification function
mapping(bytes32 => DataCert) public dataCerts;
event DataCertified(bytes32 indexed dataHash, address indexed dataOwner, address indexed receiver, uint256 timestamp);

function certData(bytes memory plainData, address receiverPubKey) public returns (bytes32) {
    bytes32 aesKey = generateAESKey();
    (bytes memory encData, bytes memory mac) = aes256GCMEncrypt(plainData, aesKey);
    bytes memory encAESKey = eccEncrypt(aesKey, receiverPubKey);
    bytes32 dataHash = sha256(abi.encodePacked(plainData, block.timestamp));

    DataCert memory cert = DataCert({
        dataOwner: msg.sender,
        dataHash: dataHash,
        encryptedAESKey: encAESKey,
        encryptedData: encData,
        mac: mac,
        timestamp: block.timestamp
    });

    dataCerts[dataHash] = cert;
    emit DataCertified(dataHash, msg.sender, receiverPubKey, block.timestamp);

    return dataHash;
}
```

(a)

```
// Data decryption and verification function
function verifyData(bytes32 dataHash, bytes memory plainData, bytes memory privateKey) public returns (bool) {
    DataCert memory cert = dataCerts[dataHash];

    require(cert.dataOwner == msg.sender, "Invalid data owner");
    require(sha256(abi.encodePacked(plainData, cert.timestamp)) == dataHash, "Data tampered");

    bytes32 aesKey = eccDecrypt(cert.encryptedAESKey, privateKey);
    bool macValid = aes256GCMDecryptVerify(cert.encryptedData, aesKey, cert.mac);

    return macValid;
}
```

(b)

**Figure 3.** On-chain storage and certification code

## (2) Design of Multi-node Communication Protocol and Process for the Platform

This paper adopts an improved Practical Byzantine Fault Tolerance (PBFT) consensus mechanism. Without the need for computing power competition, this mechanism can complete block consensus verification within 3–5 seconds, which meets the timeliness requirements of "real-time matching and efficient settlement" in green electricity transactions. Meanwhile, it supports 1/3 node fault tolerance, and is capable of resisting malicious behaviors such as data tampering and transaction forgery by malicious nodes. It is suitable for the distributed collaboration needs of four types of nodes—regulatory authorities, power generation enterprises, electricity consumers, and electricity sales companies—and achieves a balance between consensus efficiency and security. The consensus communication process of the green electricity supply-demand matching platform consists of five phases: data preprocessing → block proposal → multi-round verification → consensus confirmation → on-chain synchronization. All nodes collaborate according to the protocol to ensure that each matching transaction is traceable and tamper-proof.

- (i) Data Preprocessing and On-chain Storage Request

Data preprocessing and on-chain storage requests constitute the fundamental stages of consensus. Green electricity suppliers upload encrypted power generation data (including 15-minute power output, equipment parameters, etc.) via the DUP protocol with their private key signatures attached, while electricity consumers synchronously upload their demand data and generate corresponding data digests. After receiving the data, the nodes of electricity sales companies complete initial validity verification through signature authentication and digest comparison. Upon passing the verification, they send on-chain storage requests to the regulatory master node, thereby providing compliant data support for subsequent block construction. The entire process is completed within T<sub>0</sub>–T<sub>1</sub> seconds, ensuring the credibility of data sources.

- (ii) Block Information of the Regulatory Master Node

The block of the regulatory master node serves as the core initiator of the consensus mechanism. Acting as the master node, the regulatory authority aggregates on-chain storage requests from electricity sales companies and constructs a candidate block based on the preliminary results of supply-demand matching. This block contains key information such as block number, previous block hash, and transaction list. Subsequently, the candidate block and the "pre-prepare" instruction are broadcast to all slave nodes via the CVP protocol. This phase is completed within T<sub>1</sub>–T<sub>2</sub> seconds, which is designed to provide unified block information for multi-node verification and constitutes a critical initiating step in the consensus process.

- (iii) Slave Node Pre-verification and Feedback

Slave node pre-verification and feedback serve as the first round of validation in the consensus process. After receiving the candidate block, each slave node verifies the rationality of the matching results in accordance with the MCP protocol, while authenticating the block hash and master node signature via the CVP protocol. Nodes that pass the verification generate a "prepare" response with their own IDs and signatures and send it to all nodes; those that fail send a "reject" response specifying the reasons for the error. This phase is completed within T<sub>2</sub>–T<sub>3</sub> seconds, and problematic block information is initially screened out through distributed independent verification.

- (iv) Multi-node Consensus Confirmation

In the decision-making phase of multi-node consensus confirmation, all nodes count the number of "prepare" responses. If the number of valid responses is greater than or equal to two-thirds of the total number of nodes, each node sends a "commit" response; if insufficient, the regulatory master node revises the information with a maximum of two retries. The regulatory master node aggregates all "commit" responses, and upon reaching the threshold, generates green certificate data attached to the block via the GIP protocol to

complete the final confirmation. This phase is completed within T3–T4 seconds, and the legitimacy of the block is guaranteed through the node voting mechanism.

#### (v) On-chain Synchronization of Full Nodes

On-chain synchronization of full nodes is mainly achieved by the master node broadcasting the final block to all nodes. After verifying the integrity of the block, each node appends it to the local blockchain ledger and updates the supply-demand matching status and user credit rating synchronously. Both green electricity suppliers and consumers receive and activate the green certificate data via the GIP protocol. This entire phase is completed within T4–T5 seconds, which realizes the full-network implementation of the block and the synchronization of business status, thus concluding the consensus process.

## 5. Design of Full - Process Collaboration Mechanism

### 5.1 Selection of Experimental Samples

The experimental sample data is prototyped on the real-world scenarios of green electricity transactions in North China, China, in 2024, covering the Inner Mongolia Wind Power Base and Hebei Photovoltaic Base. Combined with industry statistical data (e.g., 2024 Green Electricity Transaction White Paper released by the National Energy Administration) and meteorological observation data (data from meteorological stations in the North China region of the China Meteorological Administration), the dataset is generated through a three-step method: basic data collection → outlier processing → scenario-specific adjustment.

#### (1) Basic Data Generation

i) Power Generation Side Data: Actual operation data of 20 typical green energy enterprises in North China (10 wind power enterprises and 10 photovoltaic enterprises) from March to May 2024 were selected, including installed capacity (2–5 MW per wind turbine, 1–3 MW per photovoltaic array), equipment efficiency (85%–90% overall efficiency for wind turbines, 22%–24% efficiency for photovoltaic modules), and historical power generation curves. Key indicators (wind speed, light intensity, power generation) were collected at 15-minute intervals, generating 96 data records per day to ensure the capture of short-term fluctuations in green energy output (e.g., wind gusts for wind power, cloud shading for photovoltaic systems).

ii) Power Consumption Side Data: Concurrent power consumption data of 40 electricity consumers (20 industrial enterprises, 10 commercial enterprises, 10 public institutions) were selected, covering peak power load (1,000–5,000 kW for industry, 500–2,000 kW for commerce, 300–1,000 kW for public institutions) and load distribution across time periods (high load from 9:00 to 22:00 for industry, 10:00 to 21:00 for commerce). Key indicators (power consumption, power load)

were collected at 30-minute intervals, generating 48 data records per day, which matches the actual sampling frequency of electricity metering devices used by most enterprises.

iii) Meteorological Data: Hourly meteorological data for the same period in 2024 from 10 national meteorological stations in North China (including Beijing, Hohhot, Shijiazhuang, etc.) were adopted, covering wind speed, wind direction, light intensity, temperature, and precipitation. These data serve as the core influencing factors for fluctuations in green energy output.

iv) Transaction and Cost Data (matching results, intermediary fees, verification time consumption): Data were aggregated at 1-hour intervals, generating 24 data records per day to balance data accuracy and statistical efficiency.

#### (2) Outlier Identification

The  $3\sigma$  principle was adopted to screen outlier data (e.g., extreme values where wind speed exceeds 25 m/s, irrational values where light intensity is less than 0), combined with industry experience-based judgments (e.g., light intensity of photovoltaic systems should be 0 at night).

Outlier Correction: For extreme meteorological data (e.g., typhoons, blizzards), correction coefficients from historical data of similar weather conditions during the same period were referenced (e.g., when wind speed exceeds 20 m/s, wind power output is converted at 90%). For equipment failure data (e.g., inverter shutdowns), missing values were filled using the formula: average value of the same period in the previous 3 days  $\times$  equipment failure rate (2% for wind power, 1.5% for photovoltaic systems).

Missing Value Imputation: Linear interpolation was used to fill short-term missing data (less than 2 hours), and the average value of the same period on adjacent days method was applied for long-term missing data (2–6 hours), ensuring data continuity.

#### (3) Scenario-specific Adjustment Rules

To simulate experimental scenarios such as extreme weather and changes in transaction scale, the basic data shall be adjusted in accordance with the following rules.

##### (i) Extreme Weather Scenarios

Gale Weather: Based on the gusty weather event in North China on April 15, 2024, the wind speed is increased by 30%–50% overall. The wind power output is adjusted as base output  $\times$  1.2, with an additional  $\pm 5\%$  random fluctuation of equipment performance superimposed.

Cloudy Weather: Based on the cloudy weather in North China on May 8, 2024, the light intensity is randomly attenuated by 20%–60% by time period (20%–30% attenuation from 10:00 to 14:00, 40%–60% attenuation from 15:00 to 17:00), and the photovoltaic power output is attenuated synchronously.

(ii) Transaction Scale Scenarios

Small-scale Scenario (10 power generators + 20 electricity consumers): 5 wind power enterprises and 5 photovoltaic enterprises, as well as 10 industrial, 5 commercial and 5 public-sector electricity consumers are randomly selected, with 50% of the core fluctuation data extracted.

Large-scale Scenario (50 power generators + 100 electricity consumers): Data for new participants are generated via the "feature replication + minor variation" method (e.g., the deviation of the wind speed-power output

curve of newly added wind power enterprises is  $\leq 5\%$ ), ensuring the consistency of data distribution.

(4) Generation of Key Indicator Data

The experiment utilizes two types of core time-series data, namely 'Wind Speed-Power Generation' for wind power enterprises (Table 2) and 'Irradiance-Power Generation' for photovoltaic (PV) enterprises (Table 3). The data is sampled from a typical period on April 10, 2024, characterized by clear skies and no extreme weather. The data granularity is 15 minutes for the generation side and 30 minutes for the consumption side.

Table 2. Sample Data of a Wind Power Enterprise

Time	Base Wind Speed (m/s)	Time-period Correction Coefficient	Final Wind Speed (m/s)	Wind Speed (m/s)	Wind Speed (m/s)	Wind Turbine Efficiency	Real-time Output (MW)	Power Generation (MWh)
08:15	6.2	0.9	5.58	3	12	88%	0.42	0.105
08:30	6.8	0.95	6.46	3	12	88%	0.58	0.145
08:45	7.5	1	7.5	3	12	88%	0.81	0.203
09:00	8.2	1.05	8.61	3	12	88%	1.08	0.27
09:15	9	1.1	9.9	3	12	88%	1.45	0.363
09:30	8.5	1.15	9.78	3	12	88%	1.4	0.35
09:45	7.8	1.2	9.36	3	12	88%	1.28	0.32
10:00	7	1.2	8.4	3	12	88%	1.02	0.255

Table 3. Partial Time-period Data of Light Intensity and Power Generation on April 10 for a Photovoltaic Enterprise (Rated Power: 2 MW)

Time	Sunrise/Sunset Time	Base Light Intensity (W/m <sup>2</sup> )	Weather Correction Coefficient	Random Fluctuation Coefficient	Final Light Intensity (W/m <sup>2</sup> )	Temperature (°C)	Temperature Coefficient	Module Efficiency	Real-time Output (MW)	15-minute Power Generation (MWh)
08:00-08:15	6:00/18:00	480	1.0 (Sunny)	0.03	494.4	18	-0.0045	23%	0.22	0.055
08:15-08:30	6:00/18:00	550	1	-0.02	539	19	-0.0045	23%	0.25	0.063
08:30-08:45	6:00/18:00	630	1	0.04	655.2	20	-0.0045	23%	0.3	0.075
08:45-09:00	6:00/18:00	720	1	-0.01	712.8	21	-0.0045	23%	0.33	0.083
09:00-09:15	6:00/18:00	820	1	0.02	836.4	22	-0.0045	23%	0.38	0.095
09:15-09:30	6:00/18:00	910	1	-0.03	882.7	23	-0.0045	23%	0.41	0.103
09:30-09:45	6:00/18:00	980	1	0.01	989.8	24	-0.0045	23%	0.44	0.11

09:45-10:00	6:00/18:00	1050	1	-0.02	1029	25	-0.0045	23%	0.46	0.115
-------------	------------	------	---	-------	------	----	---------	-----	------	-------

### 5.2. Selection of Experimental Samples

Based on the real new energy transaction data of a province in 2024, this experiment constructs a sample database covering two types of power generation entities (wind power

and photovoltaic) and three types of electricity-consuming entities (industrial, commercial, and residential). Two types of entity scales and two output fluctuation scenarios are designed to form a multi-dimensional comparative test plan. The selection of experimental samples is shown in Table 4.

Table 4. Experimental Sample Selection

Category	Specific Settings	Key Details
Subject Scale	Small-scale scenario	Power generation enterprises: 10 total (6 wind power, 4 solar PV)
		Electricity consumers: 20 total (8 industrial, 7 commercial, 5 residential)
	Large-scale scenario	Power generation enterprises: 50 total (30 wind power, 20 solar PV)
		Electricity consumers: 100 total (40 industrial, 35 commercial, 25 residential)
Output Fluctuation Scenario	Low fluctuation ( $\pm 10\%$ )	Simulation condition: Conventional weather (wind speed 5—10m/s, light intensity 800—1000W/m <sup>2</sup> )
		Output characteristic: Stable output curve
	High fluctuation ( $\pm 30\%$ )	Simulation condition: Extreme weather frequent periods (e.g., alternating strong winds, heavy rains, cloudy skies); wind speed 2-18m/s, light intensity 200-1200W/m <sup>2</sup>
		Output characteristic: Sharply fluctuating output curve
Sample Data Generation Rules	Power generation enterprises	Wind power: Peak output at wind speed 5-15m/s, linear output decline beyond this range
		Solar PV: Optimal output at light intensity 800-1200W/m <sup>2</sup> , 5%-8% conversion efficiency drop when temperature exceeds
		Data source: Hourly output curves generated with historical meteorological data and seasonal fluctuation rules
	Electricity consumers	Industrial: Peak hours 9:00-12:00, 14:00-16:00; load fluctuation $\pm 5\%$
		Commercial: Peak hours 10:00-22:00; load fluctuation $\pm 8\%$
		Residential: Peak hours 18:00-22:00; load fluctuation $\pm 10\%$
		Enhancement measure: Integrates holiday electricity fluctuation characteristics to improve sample authenticity

### 5.3. Selection of Experimental Samples

(i)Output Accuracy Prediction Analysis. Output accuracy prediction covers three typical scenarios: conventional weather (wind speed 5-10 m/s, light intensity 800-1000 W/

m<sup>2</sup>), extreme strong winds (wind speed 15-18 m/s), and cloudy low light (light intensity 200-500 W/m<sup>2</sup>). During the test, key data were recorded simultaneously: the hourly predicted output value and actual output value of the model. The adjustment effect of the correction factor  $\lambda$  (1.2-1.5) on

attention weights under extreme weather scenarios was statistically analyzed, and the inhibitory effect of the extreme error penalty mechanism on ultra-threshold errors (error > 10%) was verified. As shown in Figure 4, the experimental results indicate that the proposed model achieves a MAE of 2.3% and RMSE of 3.1% under conventional weather, a MAE of 5.8% and RMSE of 6.7% under extreme strong wind scenarios, and a MAE of 6.2% and RMSE of 7.1% under cloudy low light scenarios. Compared with the traditional ARIMA model, the error is reduced by 45%-55%, and compared with the basic LSTM model, the error is reduced by 20%-30%. Moreover, the prediction error under extreme weather is controlled within 8%, meeting the data accuracy

requirements for precise supply-demand matching. It can be concluded that the model effectively improves the output prediction accuracy under different meteorological scenarios, provides reliable data support for precise supply-demand matching, and exhibits significant advantages in the application of new energy output prediction.

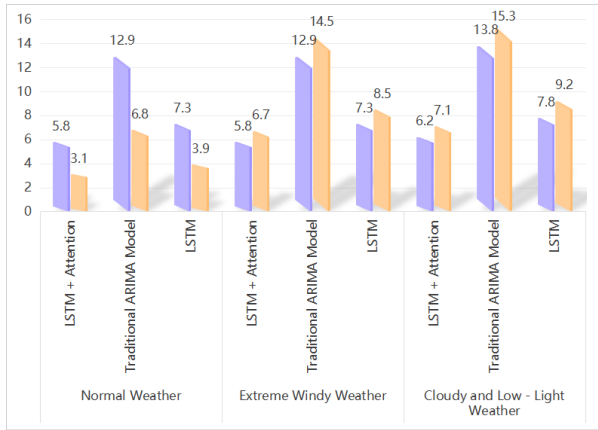
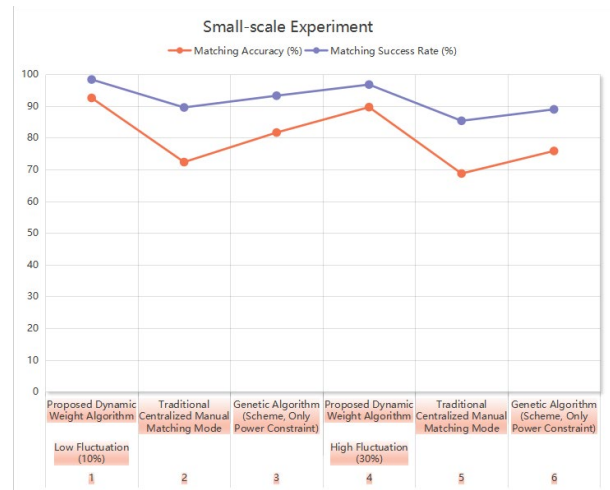


Figure 4. Output Accuracy Prediction Analysis

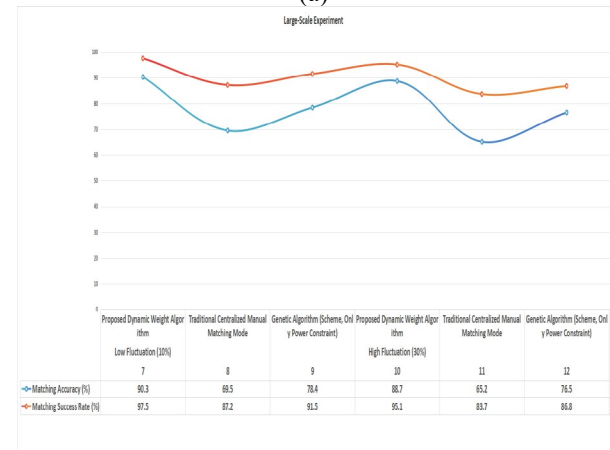
(ii) Supply-Demand Matching Efficiency Analysis. The supply-demand matching efficiency test centered on the adaptability of the dynamic weight algorithm, verifying its computational efficiency and result rationality through multi-dimensional scenario settings. The experiment was divided into small-scale (10 power generation enterprises + 20 electricity consumption enterprises) and large-scale (50 power generation enterprises + 100 electricity consumption enterprises) based on subject scale, and low fluctuation ( $\pm 10\%$ ) and high fluctuation ( $\pm 30\%$ ) based on output fluctuation. Each scenario was tested repeatedly 20 times to take the average value, with simultaneous comparisons made against the traditional centralized model and the genetic algorithm-based scheme.

As shown in Figure 5(a), the algorithm designed in this paper exhibits excellent performance in both low-fluctuation ( $\pm 10\%$ ) and high-fluctuation ( $\pm 30\%$ ) environments within small-scale scenarios: in the low-fluctuation scenario, its matching accuracy reaches 92.5% and success rate hits 98.3%, representing increases of 27.9% and 9.8% respectively compared with the traditional manual matching mode; even in the high-fluctuation environment, the algorithm still stably maintains a matching accuracy of 89.6% and a success rate of 96.7%, which are 20.9% and 11.4% higher than those of the traditional manual matching mode. This effectively reduces supply-demand mismatches caused by information asymmetry and output fluctuations.

As shown in Figure 5(b), Even in the extreme test scenario of large-scale and high-fluctuation, the algorithm still maintains a matching accuracy of 88.7% and a success rate of 95.1%, which are 15.9% and 9.6% higher than those of the genetic algorithm that only considers power constraint, highlighting the comprehensive regulatory value of dynamic weights for multi-constraints such as credit rating and regional absorption capacity.



(a)



(b)

Figure 5. Analysis of Matching Efficiency

This advantage stems from the algorithm's accurate capture of diverse demands: by quantifying the weights of various constraints through the Analytic Hierarchy Process (AHP), it not only ensures the stable power supply needs of industrial users but also balances the differences in electricity price sensitivity between commercial and residential users. In summary, the dynamic weight algorithm demonstrates efficient adaptability across scenarios with different subject scales and output fluctuations. It not only addresses the pain points of the traditional model (e.g., long time consumption) and the genetic algorithm (e.g., single-factor consideration) but also provides reliable technical support for the market-oriented and refined development of new energy transactions.

(iii) Trust Cost Analysis. Due to the lack of credible data certification and traceability mechanisms, the traditional centralized model requires entrusting third-party institutions to conduct data authenticity verification and periodic audits. This not only results in redundant processes but also makes intermediary service fees a core component of costs, forming a high-cost barrier to trust building. In terms of total costs, as shown in Figure 6, the daily average trust verification cost of the blockchain model is 1,280 yuan, representing a significant

30.8% reduction compared to the 1,850 yuan daily average cost of the traditional centralized model, demonstrating remarkable cost optimization effects. Specific experimental data: Relying on its technical architecture, the blockchain model achieves independent trust construction, with costs mainly concentrated in two core technical support items—smart contract deployment (300 yuan/day, accounting for 23.4%) and on-chain data storage (980 yuan/day, accounting for 76.6%). In contrast, the traditional model relies on third-party intermediaries to establish trust, with third-party verification fees accounting for a substantial 64.9% of the cost structure (1,200 yuan/day), while data audit fees and other expenses account for 27.0% (500 yuan/day) and 8.1% (150 yuan/day) respectively.

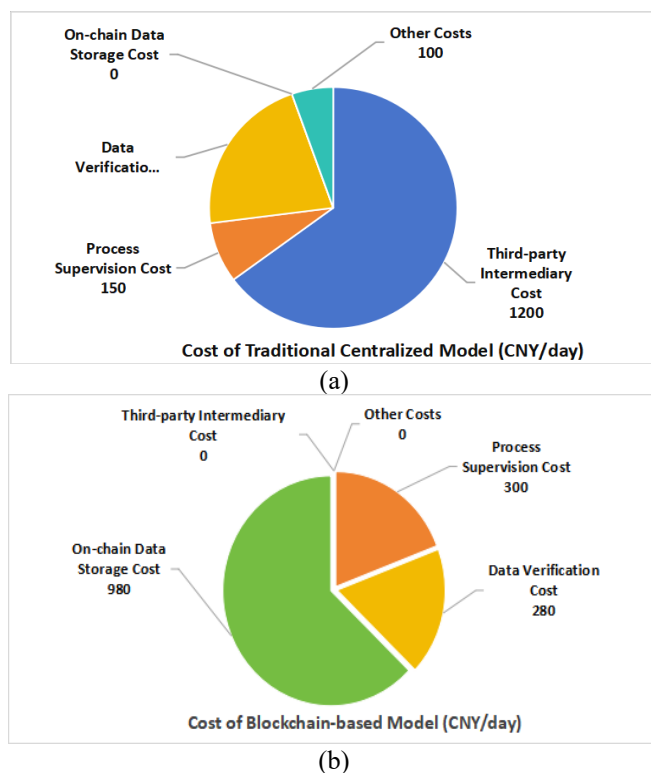


Figure 6. Trust Cost Analysis

## 6. Conclusion

This paper constructs a blockchain - based accurate new energy supply - demand matching model. Through the five - layer blockchain architecture, full - process collaboration mechanism, and multi - technology integration, it effectively solves the problems of information asymmetry, cumbersome processes, and lack of trust in new energy supply - demand matching. Simulation results show that the model performs excellently in terms of matching accuracy, transaction efficiency, and cost control. In the future, in - depth research can be carried out around the improvement of model performance and the expansion of application value. The prediction algorithm can be optimized by integrating

reinforcement learning to improve the accuracy of new energy output prediction under extreme weather. At the same time, functions such as electricity - carbon collaborative accounting and dynamic electricity price adjustment can be incorporated into the model system to consolidate the data foundation of supply - demand matching while adapting to the new needs of new energy marketization development. With the in - depth integration of blockchain technology and the new energy industry, this model is expected to be continuously improved, providing important support for building an efficient, transparent, and credible new energy market system and helping to solve more key problems in industrial practice.

## References

- [1] Zhao W, Zhang S, Xue L, et al. Research on model of micro - grid green power transaction based on blockchain technology and double auction mechanism [J]. Journal of Electrical Engineering and Technology, 2023, 19 (1): 133-145.
- [2] Smith J, Johnson L, Williams K. A consortium blockchain - based microgrid green power trading model[J]. IEEE Transactions on Sustainable Energy, 2023, 14(3): 1890 - 1901.
- [3] Müller T, Schmidt A, Weber M. Blockchain - enabled traceability system for photovoltaic power in Germany[J]. Energy Policy, 2022, 169: 113120.
- [4] Wang Peng, Liu Dunnan, Zhang Ning. Construction of blockchain - based green electricity supply - demand traceability system [J]. Power System Technology, 2021, 45(5): 1701 - 1708.
- [5] Wang Lili, Zhang Guobao, Li Jun. Research on blockchain - empowered inter - provincial green electricity transaction matching mechanism [J]. Electric Power, 2023, 56(7): 102 - 109.
- [6] Chen Qun, Li Na, Wang Hao. Green electricity output prediction model integrating blockchain and LSTM [J]. Journal of Tsinghua University (Natural Science Edition), 2024, 64(4): 321 - 328.
- [7] Tang Zhengyi. Blockchain - based microgrid power transaction matching mechanism [J]. Electric Power Automation Equipment, 2021, 41(12): 135 - 141.
- [8] State Grid Blockchain Technology (Beijing) Co., Ltd. Design and practice of "State Grid Chain" green electricity transaction traceability platform [J]. Electric Power Information and Communication Technology, 2023, 21(8): 45 - 52.